

## A THEORETICAL INVESTIGATION OF THE OLIGOMERIZATION OF ETHYLENE BY TITANIUM COMPOUNDS: THE $\text{TiMeCl}_3 \cdot \text{C}_2\text{H}_4$ SYSTEM AS A MODEL FOR A QUANTITATIVE EVALUATION OF THE COSSEE MECHANISM

P. CASSOUX, F. CRASNIER and J.-F. LABARRE

*Laboratoire de Chimie de Coordination du CNRS, 205, route de Narbonne, 31030 Toulouse, Cédex (France)*

(Received July 13th, 1978)

### Summary

A quantitative evaluation of the Cossee mechanism is performed on the  $\text{TiMeCl}_3 \cdot \text{C}_2\text{H}_4$  system. Differential electron density contours maps are found to be more reliable than HOMO electron density maps for the description of ethylene insertion into the Ti–C bond. Cossee's " $\phi_{\text{RM}}$ " assumption appears to be valid in this case while the " $\pi$ -back bonding" formulation seems improbable. The existence of a "four centre intermediate" is related to the magnitude of the activation barrier to insertion.

### Introduction

The mechanism of Ziegler–Natta catalysis of polymerization of  $\alpha$ -olefins proposed by Cossee in 1964 [1] is the most generally accepted. The basic assumptions of this mechanism were the following: (a) the trigonal bipyramidal structure of a hypothetical  $\text{TiRCl}_4$  compound is distorted in a first step towards an octahedral model situation in which a vacant site is created in an equatorial position; (b) an ethylene molecule is coordinated into the vacant site and the HOMO (highest occupied molecular orbital),  $\phi_{\text{RM}}$ , of the formed octahedral complex,  $\text{TiRCl}_4 \cdot \text{C}_2\text{H}_4$ , relates to the bond between alkyl group and Ti, (c) the energy gap between  $\phi_{\text{RM}}$  and the LUMO (lowest unoccupied molecular orbital), the latter representing a combination of the  $d_{vz}$  orbital and the  $\pi^*$  antibonding of ethylene, is appreciably reduced. It is now easier to promote an electron from  $\phi_{\text{RM}}$  into the LUMO by thermal excitation, and (d) the MR bond is more susceptible to breaking and the alkyl group will be expelled as a radical which attaches itself to the nearest C atom of the ethylene, while the other C atom becomes attached to the titanium in a concerted process involving a four centre transition state.

At the time of his mechanistic proposal, Cossee could not offer any experimental or theoretical proof of this assumptions. UV photoelectron spectroscopy was inadequately developed and quantum calculation methods for ground and excited states of transition metals complexes were not available. More recently, calculations on similar "soluble" catalysts, assumed to be formed from the combination of titanium and aluminium compounds, have been performed by Perkins [2], Novaro [3] and Clementi [4].

In a previous paper [5], we reported the photoelectron spectra, of some  $\text{TiRX}_3$  compounds ( $R = \text{Me}$ ;  $X = \text{Cl, Cp, OR, NR}_2$ ) and their assignments made with the aid of the "extended CNDO" method. The first band observed in the spectrum of these compounds corresponds to the Ti—C bond orbital only in the case of  $\text{TiMeCl}_3$ , considerable mixing occurring for cyclopentadienyl, alkoxy and dialkyl-amino derivatives between Ti—C bond orbitals and Cp, O and N orbitals, respectively. In other words, the  $\phi_{\text{RM}}$  assumption (b) appeared to be acceptable only for  $\text{TiMeCl}_3$ . On the other hand, the ionization potentials attributed to the Ti—C bond orbital lie in the range 9.8–10.8 eV: this would mean that, following Koopmans theorem [6], the energy gap between the HOMO and the LUMO would be ca. 10 eV, i.e. 230 kcal/mol. Under such conditions, whatever the magnitude of the effect resulting from coordination of ethylene, such an energy gap would seem to make assumption (c) improbable.

However one of these compounds,  $\text{TiMeCl}_3$ , for which the  $\phi_{\text{RM}}$  assumption (b) is correct, is a moderately active monomeric, soluble catalyst for which there is little doubt that titanium(IV) centers are involved [7]. We therefore decided to study the  $\text{TiMeCl}_3 \cdot \text{C}_2\text{H}_4$  system thoroughly in order to better understand the origin of the catalytic activity of titanium(IV) compounds and to assess the validity of a Cossee-type mechanism when extended to this simple model for a soluble catalyst.

### Computational techniques

All valence electron MO-SCF calculations were carried out by the Extended CNDO method [8]. In an earlier paper [5] we proposed for titanium a set of optimized orbital exponents  $\alpha$  and  $\beta$  parameters:  $\alpha_{4s} 1.260$ ;  $\beta_{4s} -12.0$ ;  $\alpha_{4p} 0.375$ ;  $\beta_{4p} -10.0$ ;  $\alpha_{3d} 2.24$ ;  $\beta_{3d} -19.0$ . These values were consistent with those previously reported for Ni, Fe, Cr [9].

The geometry of  $\text{TiMeCl}_3$  being unknown, the calculations were performed on a partially optimized Pople and Gordon's standard model [10]:  $d(\text{Ti—C}) 2.15 \text{ \AA}$  (optimized);  $d(\text{Ti—Cl}) 2.17 \text{ \AA}$  (as in  $\text{TiCl}_4$  [11]);  $d(\text{C—H}) 1.10 \text{ \AA}$ ; tetrahedral angles assumed all equal on Ti. These bond lengths were kept constant when passing to the various model situations which will be further described, only the valency angles being varied. On doing this, we observed that the non bonding bicentric energy terms, as defined by Pople [12], involving the chlorine atoms, namely  $E(\text{Cl}\cdots\text{Cl})$  and  $E(\text{C}\cdots\text{Cl})$ , were, as previously noted [13], overestimated. This arises from the evaluation of the semi-empirical bonding parameters  $\beta_{\text{AB}}^0$  [14]:

$$\beta_{\text{AB}}^0 = \frac{1}{2}K(\beta_{\text{A}}^0 + \beta_{\text{B}}^0)$$

in which the constant  $K$  is generally taken as 0.75 for elements of the first and

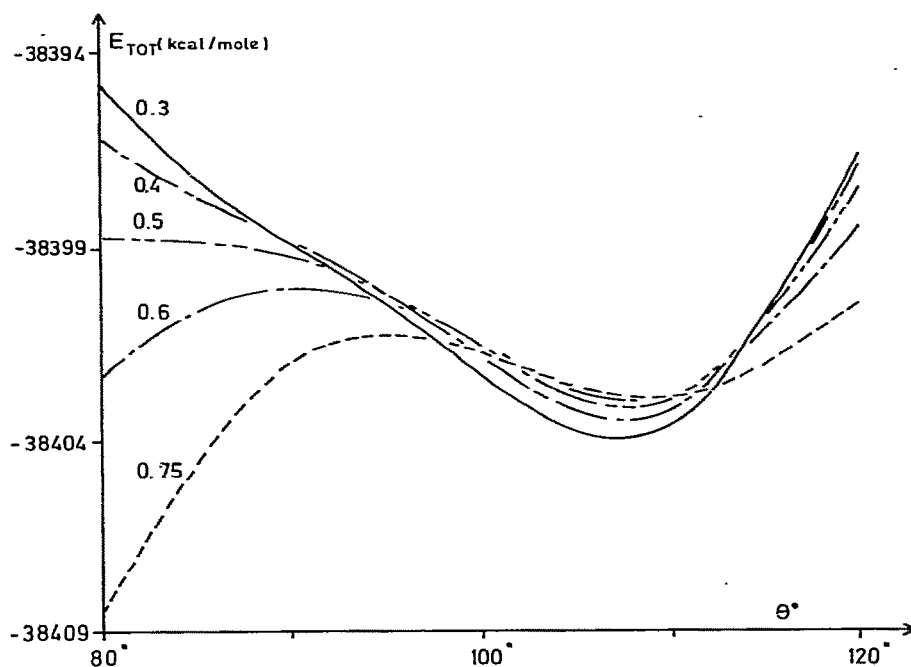


Fig. 1. Total energy ( $E_{TOT}$ ) of  $TiMeCl_3$  vs. The  $CTiCl$  angle ( $\theta$ ) for various  $K$  values.

second rows of the periodic table. Using this 0.75 value the potential curve for  $TiMeCl_3$  (Fig. 1) exhibits not only the expected energy well for  $\theta$  ( $CTiCl$ ) close to  $109.47^\circ$ , but also a very sharp decrease for  $\theta$  values smaller than  $90^\circ$ , i.e. in an area where the  $E(C\cdots Cl)$  interaction terms would have to be repulsive and consequently would destabilize the system. The  $K$  parameter was refined and a correct potential curve with an unique well for  $\theta \simeq 109.47^\circ$  was obtained for a value of  $K = 0.30$  (Fig. 1), which was used in the present work. We have also checked that changing  $K$  from 0.75 to 0.30 did not significantly perturb either the sequences of the energy levels or the charge distributions.

The total and differential molecular electron density contours maps were drawn following the specifications of Roux et al. [15] and using the eigenvectors desorthogonalized by the procedure of Löwdin [16].

### Quantitative evaluation of the Cossee mechanism in the case of the $TiMeCl_3 \cdot C_2H_4$ system

#### A. Formation of a vacant site in the pentahedral coordination sphere of titanium

A vacant site on the titanium atom of  $TiMeCl_3$  can be formed by going from coordination IV to coordination V as in the trigonal bipyramid or square pyramid models visualized in Fig. 2. The total energy,  $E_{TOT}$ , was computed for each moiety and model 1 appears to be the most stable throughout the series. It is noteworthy that the energy of model 1 is only 7.2 kcal/mol higher than for tetrahedral  $TiMeCl_3$ . It is attractive, therefore, to account for the formation of a vacant site in the axial position of a trigonal bipyramid as arising from this small energy gap.

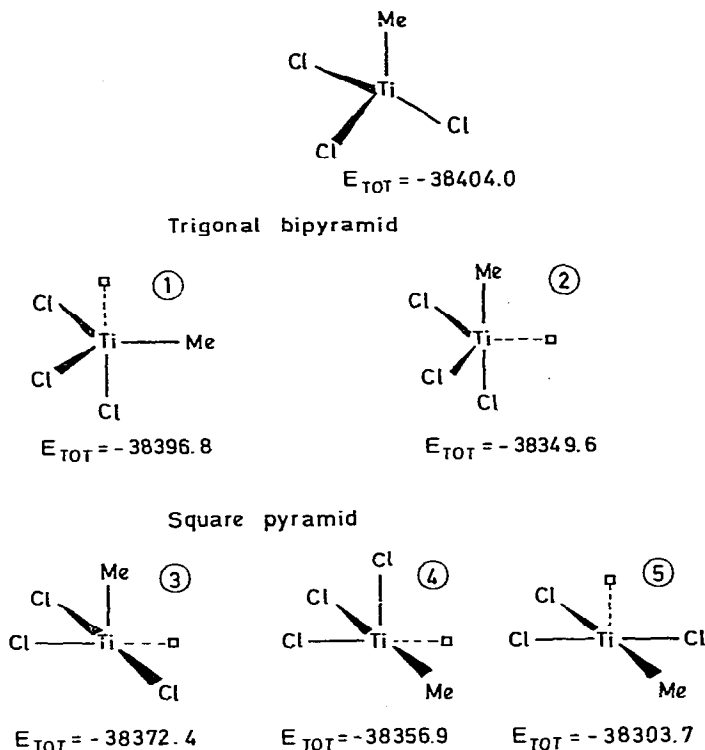


Fig. 2. Total energy ( $E_{TOT}$ ) values of tetrahedral  $TiMeCl_3$  and distorted trigonal bipyramid and square pyramid model situations.

### B. Reaction path of ethylene coordination

The approach of the ethylene to the vacant site of model 1, the C=C bond remaining parallel to the Ti—Me bond, has been examined in several steps by calculating the total energy of this hypersystem as a function of two parameters: (i) the  $d(Ti-G)$  distance from Ti to the centre of gravity of  $C_2H_4$  and (ii) the  $d(C-C)$  distance in ethylene. The potential energy well of this hypersurface was obtained for:  $d(Ti-G)$  3.55 Å, and  $d(C-C)$  1.324 Å;  $E_{TOT}$  -49145.2 kcal/mol\* (Fig. 3).

It will be noticed that  $d(C-C)$  in the complex is almost equal to the C=C bond length in free ethylene as optimized by CNDO/2 (1.310 Å [17]). Also of interest is the very large value of  $d(Ti-G)$  compared to the corresponding distance (2.09 Å) experimentally measured in the *trans*-[Pt( $C_2H_4$ )]{NH(CH<sub>3</sub>)<sub>2</sub>}Cl<sub>2</sub>, in which incidentally,  $d(C-C)$  is equal to 1.47 Å [18]. These results are consistent with a very smooth complexation of ethylene with  $TiMeCl_3$  when compared to the strong coordination observed in the stable platinum complex.

Furthermore, a detailed analysis of the electronic structure of the  $TiMeCl_3 \cdot C_2H_4$  system shows that the  $d_{yz}$  orbital population of titanium is equal to zero, as it is in  $TiMeCl_3$ -model 1. This result does not support the “ $\pi$ -back

\* The total energies of the systems resulting from the approach of ethylene to the other model situations were found to be energetically less favoured.

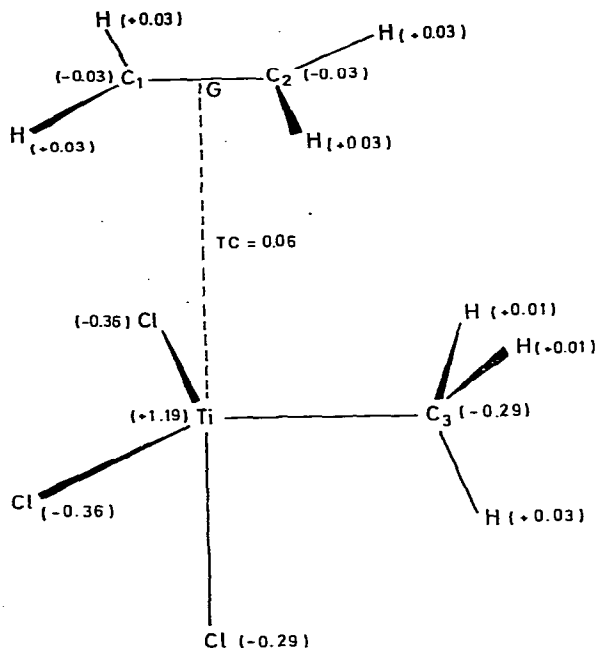


Fig. 3. The optimized  $\text{TiMeCl}_3 \cdot \text{C}_2\text{H}_4$  hypersystem (numbers in parentheses are net charges).

donation to the  $\pi^*$  of ethylene" formulation which was taken into account in the Cossee mechanism (assumption c; vide supra). Perkins et al. [2] reached the same conclusion from their quantum calculations on a titanium—aluminium—ethylene complex, whereas the reverse conclusion was obtained by Ros et al. [19] in their study of ethylene complexation to a titanium fluoride crystal.

On complexation the ethylene molecule in total loses 0.06 electrons, which are transferred to the titanium atom. This extremely weak charge transfer is illustrated by the comparison of the differential molecular electron density contours maps\* for model 1 + free ethylene at a distance of 3.55 Å (Fig. 4a) and for the real  $\text{TiMeCl}_3 \cdot \text{C}_2\text{H}_4$  system (Fig. 4b): the contours are extremely similar for both maps except perhaps for the small contraction of the line +0.001 along the Ti—G direction.

In conclusion, all the indications are against formation of a real  $\sigma$ -bond between ethylene and Ti in the  $\text{TiMeCl}_3 \cdot \text{C}_2\text{H}_4$  system. This is in agreement with the conclusions of Clementi et al. [4] about the weak binding of ethylene to Ti in the  $\text{TiCl}_4 \cdot \text{Al}(\text{CH}_3)_3$  Ziegler—Natta catalyst.

The total energy of the  $\text{TiMeCl}_3 \cdot \text{C}_2\text{H}_4$  "complex" is found to be lower by 38.4 kcal/mol than the sum ( $E_{\text{TOT}}$  (Model 1) +  $E_{\text{TOT}}$  (free  $\text{C}_2\text{H}_4$ )). This large energy difference appears to conflict with the above conclusion, but it should be noted that the CNDO approach is well known to overestimate bond energies

\* It should be noted that positive density contours correspond to regions where electron gain is observed while negative contours correspond to electron deficiency.

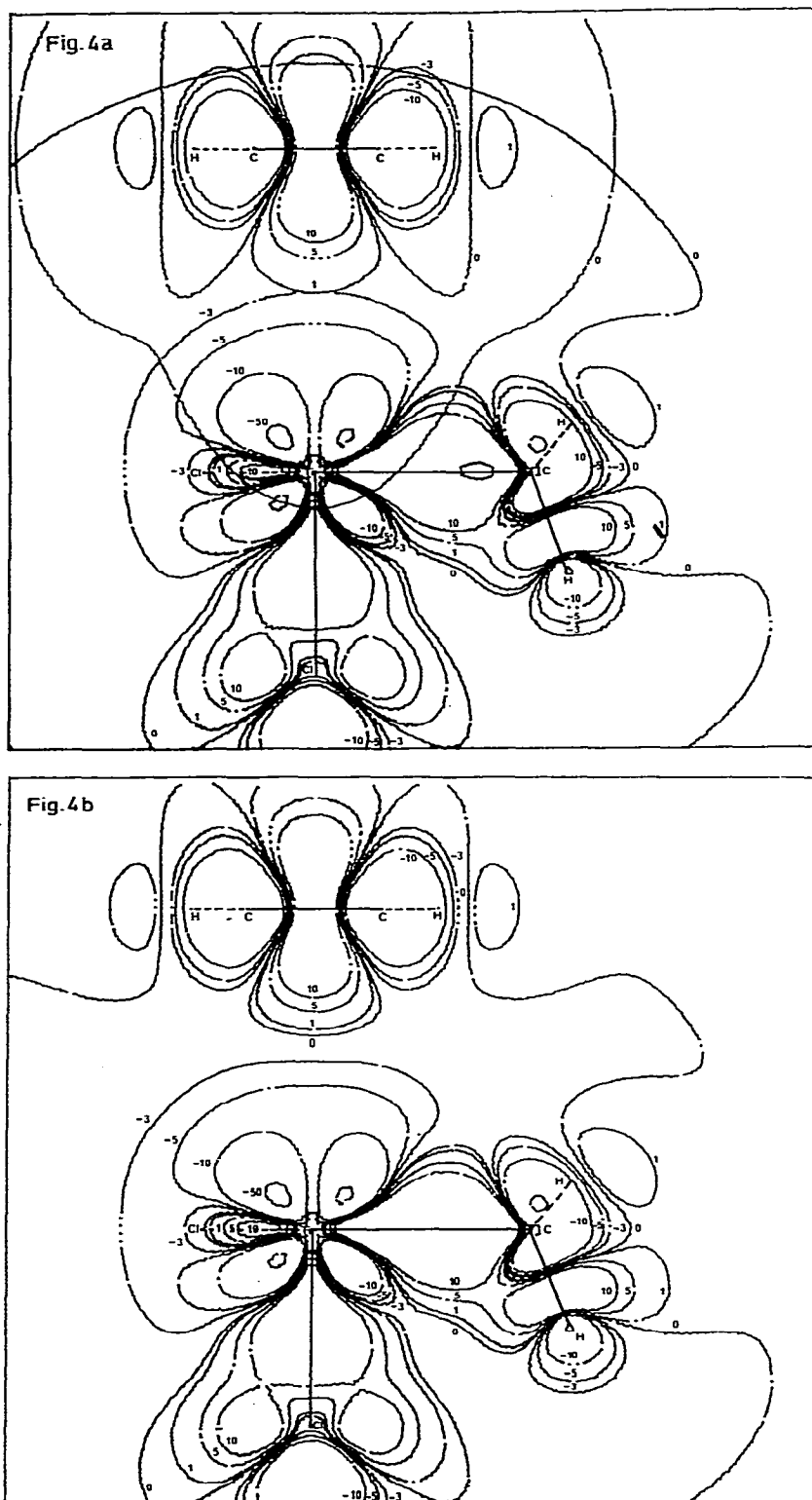


Fig. 4. Differential electron density contours maps for (a) model 1 + free C<sub>2</sub>H<sub>4</sub> ( $d(\text{Ti-G})$  3.55 Å) and (b) for the real TiMeCl<sub>3</sub> · C<sub>2</sub>H<sub>4</sub> system. (electron density in  $10^3 \text{ e au}^{-3}$ ).

[20], and this must be kept in mind in considering other energy gaps of that kind.

### C. Insertion of ethylene

The total energy for the various steps of the insertion of ethylene into the Ti—Me bond was calculated, as shown in Fig. 5, with  $\text{TiMeCl}_3 \cdot \text{C}_2\text{H}_4$  “complex” II as the initial stage. The final state III, i.e. the propyl species within the Cossee mechanism, is found to be 131.8 kcal/mol more stable than the initial complex II, the vacant site being now in the equatorial position. This model III, however, is not expected to be the most favourable because of steric hindrance induced by the methyl group. As a matter of fact a more stable conformation (by 10.1 kcal/mol) is obtained by a  $2\pi$  rotation of the Me group around the C—C bond (model IVa). Furthermore, as noted in paragraph A, the most stable situation is that in which the vacant site is in axial position. Our calculations confirm that

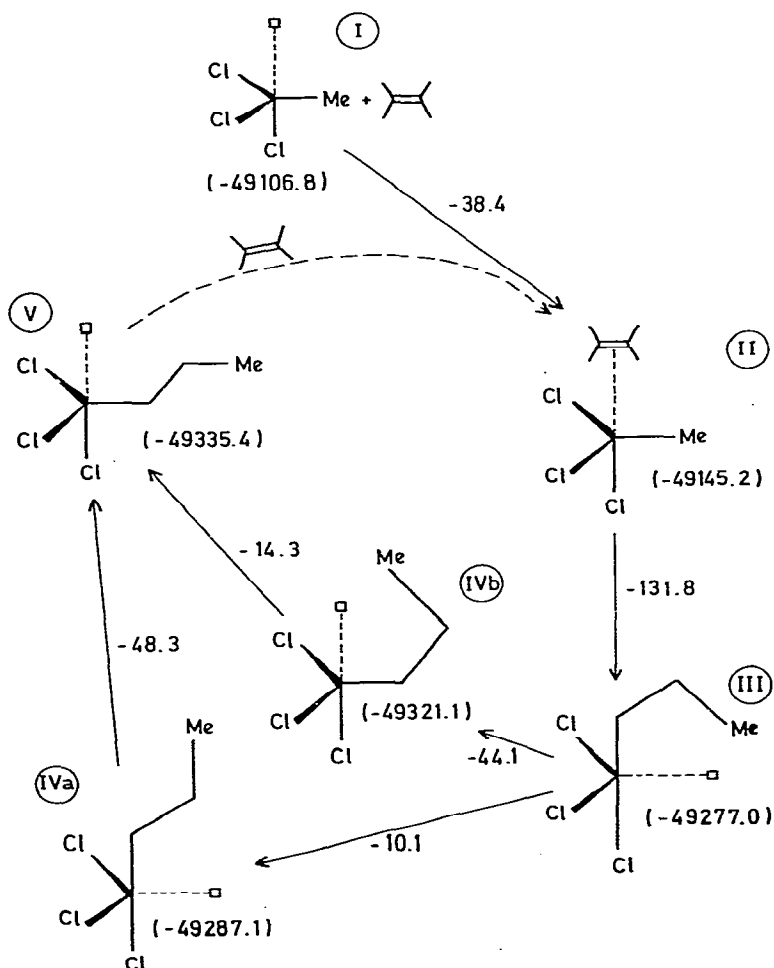


Fig. 5. Thermodynamical cycle for ethylene insertion (numbers in parenthesis are  $E_{TOT}$  values in kcal/mol).

such a model, obtained by an intramolecular rearrangement of model IVa to model V, is more stable by 48.3 kcal/mol. Alternatively a second route, involving initially an equatorial-axial reorganization (model IVb) followed by a rotation of the methyl group, can be envisaged.

Which path is considered (III  $\rightarrow$  IVa  $\rightarrow$  V or III  $\rightarrow$  IVb  $\rightarrow$  V) the reaction runs sequentially downhill energy-wise and the "driving force" as defined by Perkins [2] for the insertion of ethylene seems consequently to be the tendency for the system to go to the state of lowest energy, i.e. a propyl species which may now complex a new ethylene molecule on its axial vacant site to continue the process of oligomerization.

The cycle described in Fig. 5 is thermodynamically in favour of an extended Cossee-type mechanism\*, but this description of the catalytic cycle can be questioned. One can argue that, even if model III is more stable than model II, for example, the system may not necessarily pass from II to III, especially because there may be a large activation barrier. Detailed studies would have then to be performed for all the steps of Fig. 5. This work focuses on the II  $\rightarrow$  III reaction path because of the cost of such detailed studies and because this step is critical for discussion of the Cossee mechanism.

#### Detailed analysis of the II $\rightarrow$ III reaction path

Seven intermediates were studied for the postulated reaction path from II to III. The interatomic distances C(1)-C(2) in ethylene, C(2)-C(3)(Me), Ti-C(1) and Ti-C(3) were varied in eight equal and simultaneous steps. The results of these calculations may be depicted in two ways, (i) by the HOMO electron density contours maps which are shown for five points of the reaction in Fig. 6-10 and (ii) by the molecular differential density contours maps shown in Fig. 11-15. The HOMO of the initial complex II is, as expected, essentially connected to the Ti-C(3) (Me) bond (Fig. 6). During the migration of the methyl group (Fig. 7-9) a progressive delocalization of the electron density on the Ti, C(1), C(2) and C(3) atoms becomes apparent and finally in model III (Fig. 10) the HOMO represents now essentially the Ti-C(1) (propyl) bond with some contributions from the C(1), C(2) and C(3) atoms. The contribution in the HOMO of the titanium  $d_{yz}$  orbital, which is zero in II, increases, reaches a maximum for the fifth intermediate, and decreases again to zero in the final III. The  $d_{yz}$  orbital could be thus considered responsible for the generation of the system without bond rupture at any time. This role was described by Perkins in this study on a titanium-aluminium-ethylene compound [2] as a "transfer agent function". However, such a description based on the sole HOMO maps may be questioned: the bonding between the methyl carbon and the  $d_{yz}$  orbital, initially forbidden in II, is induced by the new symmetry of the system and this is related to the observed increasing contribution of the  $d_{yz}$  orbital. Moreover, the existence of a four centre transient state, which is essential in the Cossee mechanism, never clearly appears throughout Fig. 6-10.

(continued on p. 313)

\* In agreement with Clementi et al., [4] who observed that thermal energy (30-40 kcal/mol) must be released when such an insertion occurs, although as noted above, our  $\Delta E_{TOT}$  values are substantial overestimates.



Fig.6

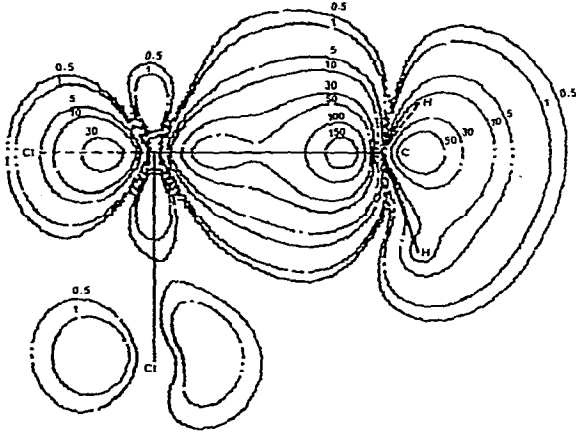
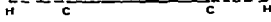


Fig.7

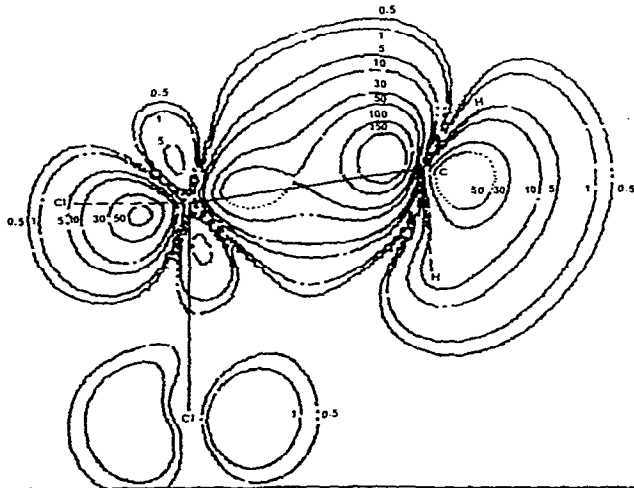
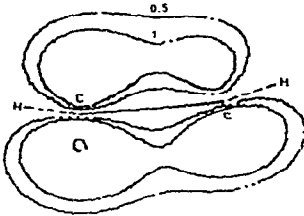


Fig. 8

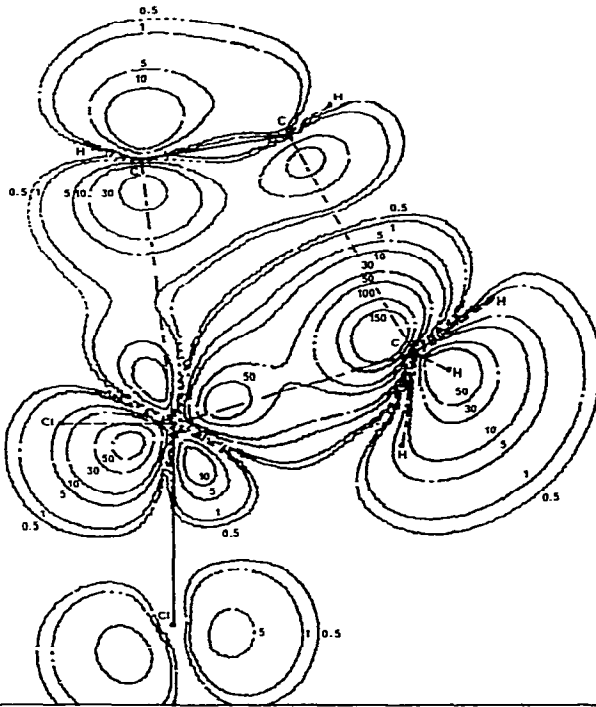
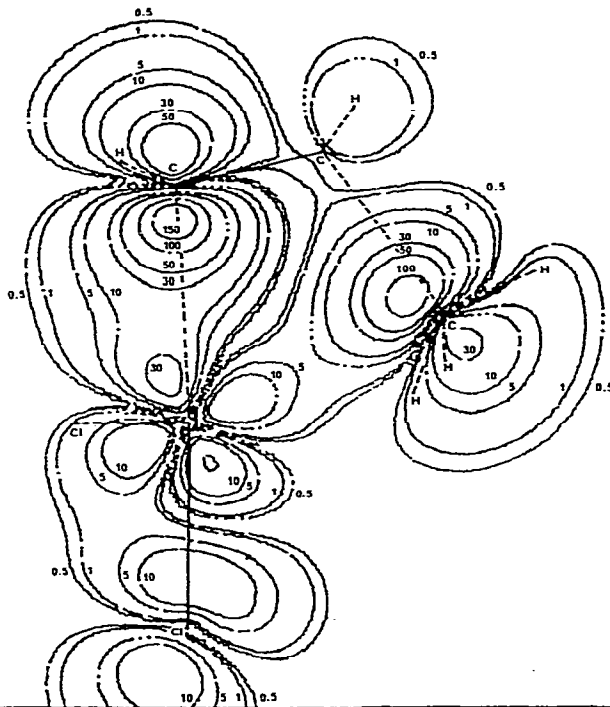


Fig. 9



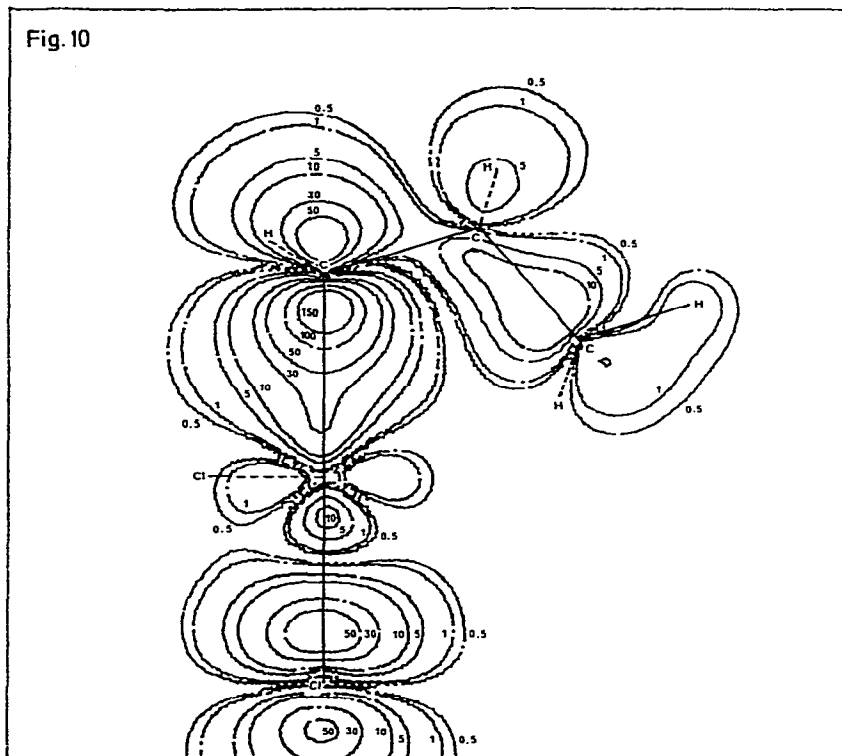


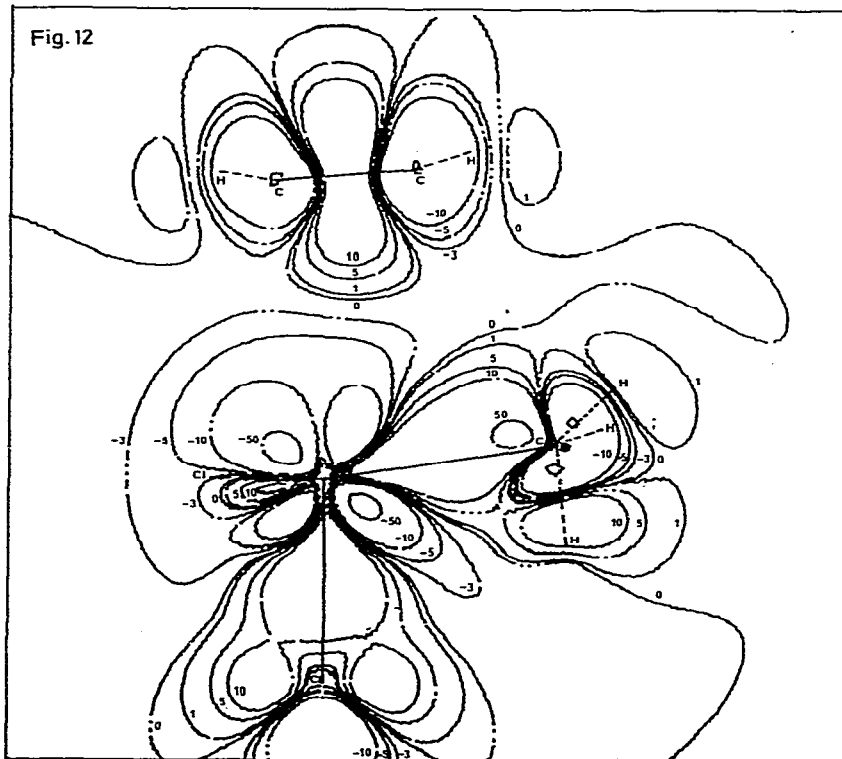
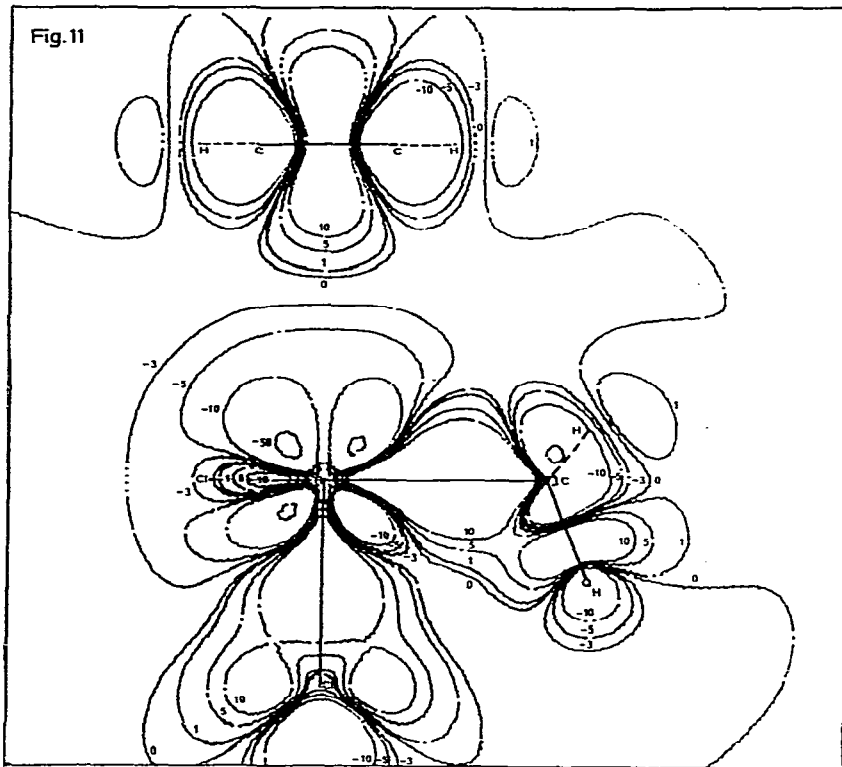
Fig. 6–10: HOMO electron density contours maps for the five steps of ethylene insertion (electron density in  $10^3 \text{ e au}^{-3}$ ) (see also the two previous pages).

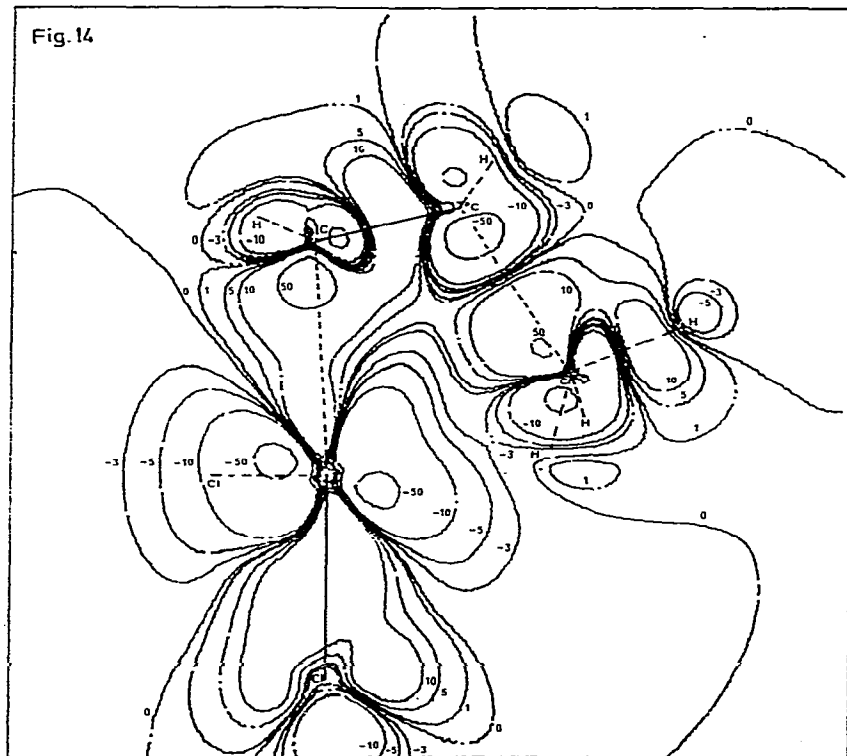
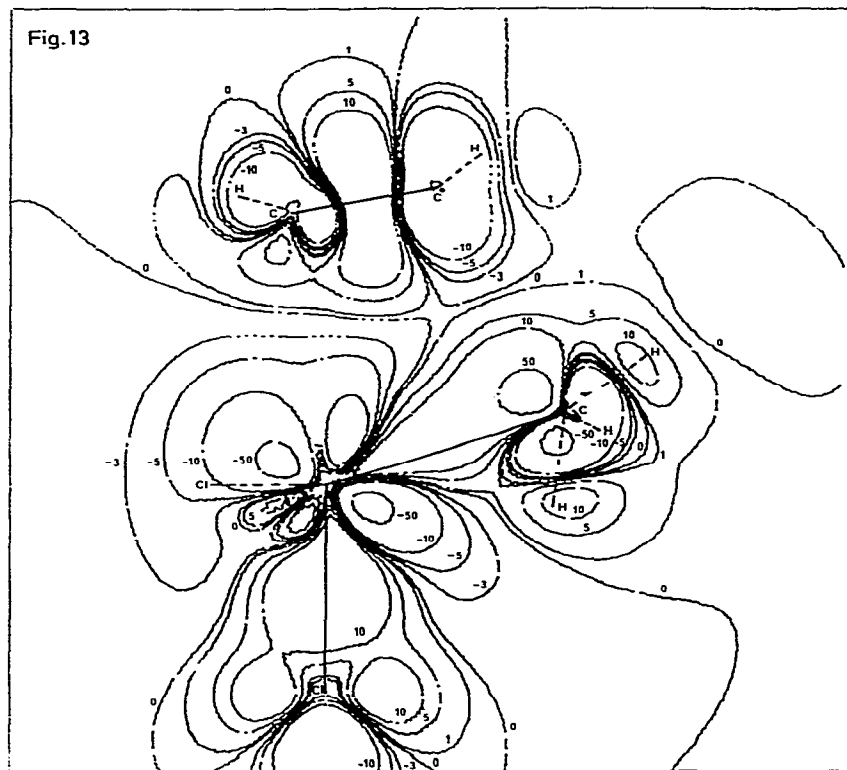
*What happens when the ethylene insertion is depicted by using the differential density description (Fig. 11–15)?*

In the differential density map of II (Fig. 11) the Ti–C(3) bond is clearly shown and is polarized towards C(3). This is in agreement with the net charges of titanium (+1.19) and C(3) (–0.29), respectively. There is no visible interaction between C(3) and C(2). In the next stage (Fig. 12), the centre of gravity of the Ti–C(3) electron pair is shifted towards the C(2)–C(3) axis. This shift is more pronounced in Fig. 13; the C(2)–C(3) and Ti–C(1) bonds are formed and this stage may be considered as the Cossee four centre intermediate. In Fig. 14, the Ti–C(3) bond vanishes and the propyl group attached to titanium is formed at the same time, and in the final situation (Fig. 15) III looks very similar to the initial situation II with a Ti–C(1) (propyl) bond polarized towards C(1), but the C(1)–C(2) and C(2)–C(3) bonds are now properly depicted.

The differential density maps appear to be much more convenient than the HOMO density maps for the description of the change in electron density in the bonds induced by molecular reorganizations analogous to those proposed by Cossee. However, these differential density maps do not provide any clear proof of the reasons why the insertion of ethylene follows the Cossee reaction path. In model II the net charges on C(3) (–0.29) and C(2) (–0.03) are both negative, and do not predispose these atoms towards an attractive interaction which would

(continued on p. 317)





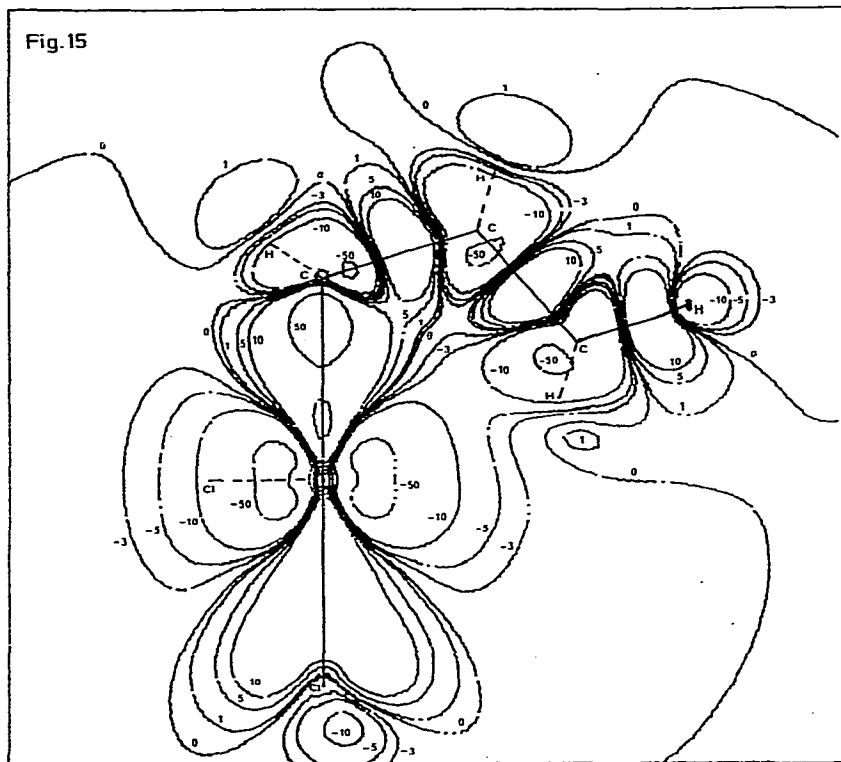


Fig. 11–15. Differential electron density contours maps for the five steps of ethylene insertion (electron density in  $10^3 e \text{ au}^{-3}$ ) (see also the two previous pages).

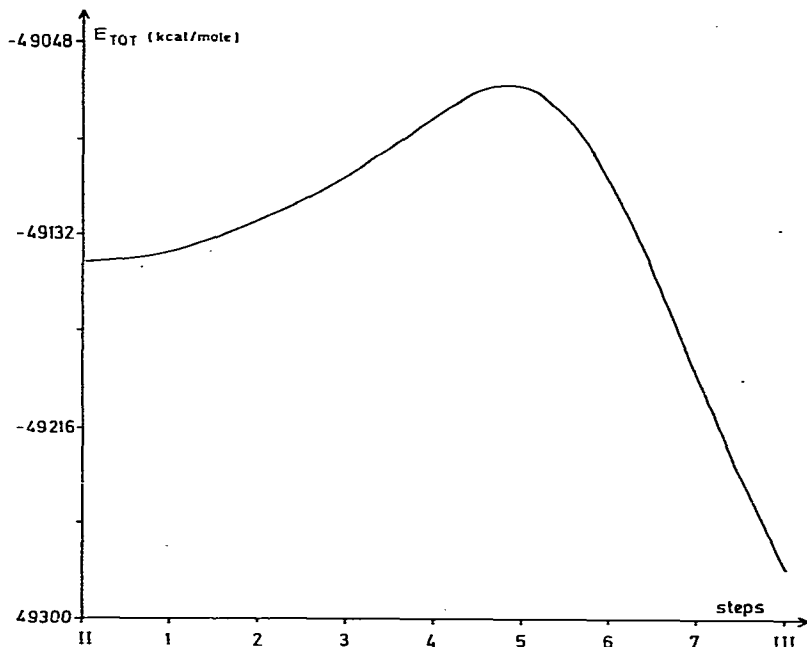


Fig. 16. The activation barrier under ethylene insertion (model II  $\rightarrow$  model III).

initiate the reaction. As a matter of fact, the corresponding  $E(C(2)\cdots C(3))$  energy term is positive in II (+0.9 kcal/mol) and remains repulsive up to the stage depicted in Fig. 13, where it becomes attractive (−27.7 kcal/mol). Furthermore, there is an activation barrier of +76 kcal/mol on going from II to III (Fig. 16). Even if this value is, as discussed above, considerably overestimated, it nevertheless corresponds to half of the energy gain (138.1 kcal/mol) from II to III. It is interesting to note that these two observations are in conflict with the interpretation favoured by Perkins [2] and Clementi [4], and they may be related to the moderate activity of  $TiMeCl_3$  as a catalyst for olefins oligomerization.

## Conclusion

This quantitative assessment of the Cossee mechanism for the activity of the monomeric soluble catalyst  $TiMeCl_3$  has demonstrated that in this case differential electron density contours maps are more reliable than those based on HOMO electron density contours. The results of the calculations on the initial complex  $TiMeCl_3 \cdot C_2H_4$  are in agreement with the  $\phi_{RM}$  assumption only when there are no alkoxy, dialkylamino or Cp groups linked to titanium. The concept of  $\pi$ -back bonding from the titanium  $d_{yz}$  orbital to the  $\pi^*$  orbitals of ethylene is disfavoured. UV photoelectron data and calculations show that the assumed promotion of an electron from  $\phi_{RM}$  to the LUMO is improbable. The four centre intermediate proposed by Cossee may be a good pattern, although there are no obvious reasons for its formation. Furthermore the magnitude of the activation barrier which may exist when this intermediate is formed must play a critical role, and this has not been considered in previous studies. Thus, even if the Cossee mechanism can be used with partial success, in some special cases, in which some of his assumptions happen to be correct, its general use for interpreting soluble catalyst activity is not justified.

## Acknowledgment

The authors are gratefully indebted to Dr. J.M. Savariault and Mr. J. Aussoleil for help and discussions on the electron density contours maps aspect of this work.

## References

- 1 P. Cossee, *J. Catal.*, **3** (1964) 80.
- 2 D.R. Armstrong, P.G. Perkins and J.J.P. Stewart, *J. Chem. Soc. Dalton Trans.*, (1972) 1972.
- 3 O. Novaro, S. Chow and P. Magnouat, *J. Catal.*, **42** (1976) 131.
- 4 G. Giunchi, E. Clementi, M.E. Ruiz-Vizcaya and O. Novaro, *Chem. Phys. Lett.*, **49** (1977) 8.
- 5 M. Basso-Bert, P. Cassoux, F. Crasnier, D. Gervais, J.F. Labarre and Ph. De Loth, *J. Organometal. Chem.*, **136** (1977) 201.
- 6 T. Koopmans, *Physica (Utrecht)*, **1** (1934) 104.
- 7 (a) H. Bestian and K. Clauss, *Angew. Chem. Int. Ed. Engl.*, **2** (1963) 704; (b) K. Kühlein and K. Clauss, *ibid.*, **8** (1969) 387.
- 8 A. Serafini, M. Pellissier, J.M. Savariault, P. Cassoux and J.F. Labarre, *Theoret. Chim. Acta*, **39** (1975) 229.
- 9 J.M. Savariault, A. Serafini, M. Pellissier and P. Cassoux, *Theoret. Chim. Acta*, **42** (1976) 155.
- 10 J.A. Pople and M.S. Gordon, *J. Amer. Chem. Soc.*, **89** (1967) 4253.
- 11 H. Uehara and Y. Morino, *J. Chem. Phys.*, **45** (1966) 4543.

- 12 J.A. Pople and D.L. Beveridge, *Approximate MO Theory*, McGraw-Hill, New York, 1970, p. 67.
- 13 G. Robinet, Ph. D. Thesis, Toulouse, No. 519, 1972.
- 14 J.A. Pople and D.L. Beveridge, *Approximate MO Theory*, McGraw-Hill, New York, 1970, p. 79.
- 15 M. Roux, S. Besnainou and R. Daudel, *J. Chim. Phys.*, 53 (1956) 218.
- 16 P.O. Löwdin, *J. Chem. Phys.*, 18 (1950) 365.
- 17 J.A. Pople and D.L. Beveridge, *Approximate MO Theory*, McGraw-Hill New York, 1970, p. 106.
- 18 P.R.H. Alderman, P.G. Owston and J.M. Rowe, *Acta Cryst.*, 13 (1960) 149.
- 19 E.J. Baerends, D.E. Ellis and P. Ros, *Theoret. Chim. Acta*, 27 (1972) 339.
- 20 M.J.S. Dewar and C.A. Ramsden, *Chem. Commun.*, (1973) 668.